

Supporting Information

Mapping of Bernal and non-Bernal
Stacking Domains in Bilayer Graphene
Using Infrared Nanoscopy

*Gyuil Jeong^a, Boogeon Choi^a, Deok-Soo Kim^a, Seongjin Ahn^b, Baekwon Park^a, Jin Hyoun
Kang^a, Hongki Min^b, Byung Hee Hong^a, and Zee Hwan Kim^{*a}*

^aDepartment of Chemistry, Seoul National University, Seoul 08826, Korea

^bDepartment of Physics and Astronomy, Seoul National University, Seoul 08826, Korea

A. Examples of IR-sSNOM images of bilayer graphene (BLG)

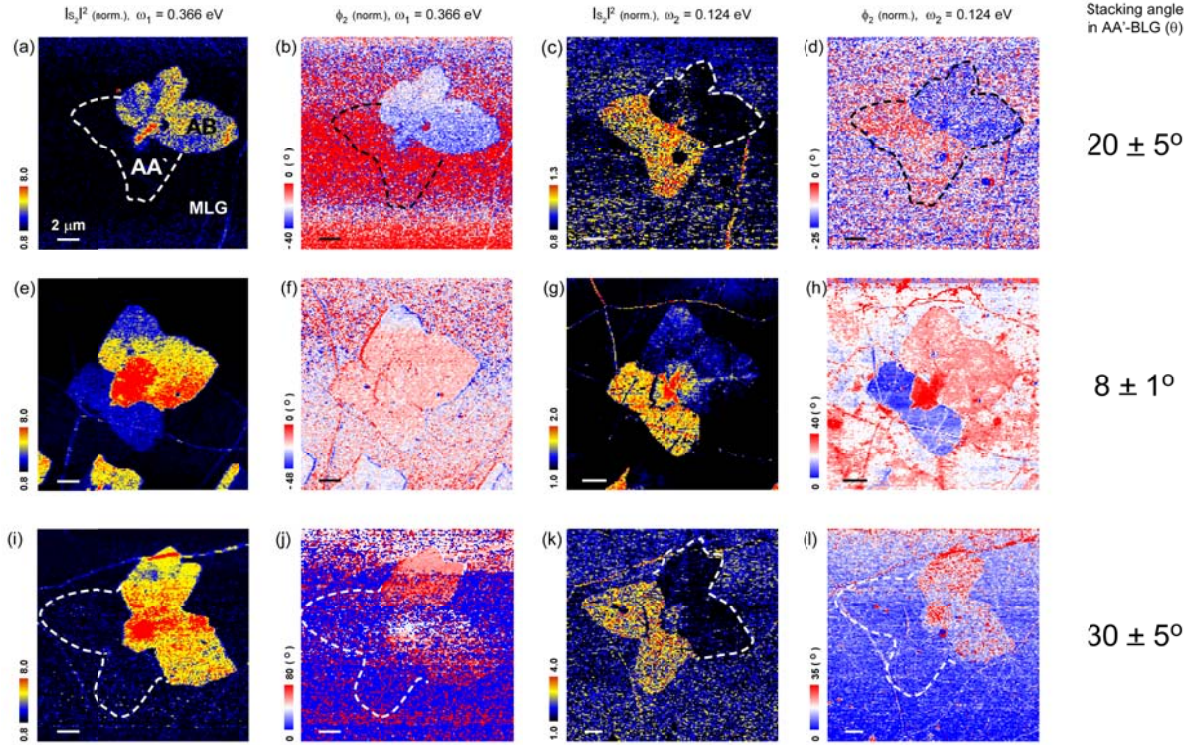


Figure S1. Examples of sSNOM intensity ($|s_2|^2$) and phase (ϕ_2) images of BLG obtained with IR light at $\omega_1 = 0.366$ eV and $\omega_2 = 0.124$ eV. The scale bars correspond to $2 \mu\text{m}$. Last column shows the stacking angles (θ) of AA'-BLG in each image, estimated from the Raman spectra (see Supporting Information-B).

B. Raman spectroscopy on AB and AA'-stacked bilayer graphene

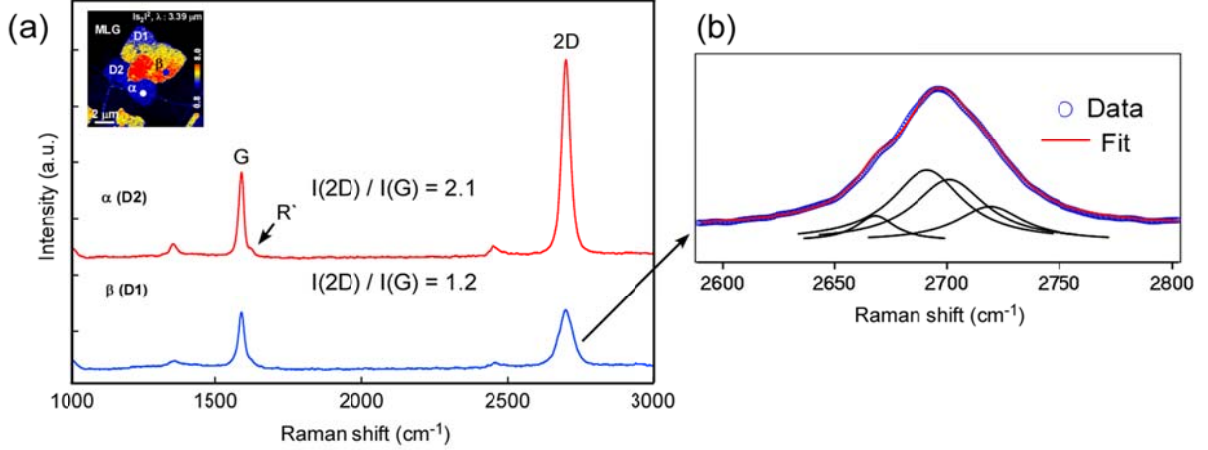


Figure S2. (a) The Raman spectra of a BLG on SiO₂/Si substrate (excitation wavelength of $\lambda_{\text{ex}} = 514.5$ nm) obtained from the D1 (β) and D2 (α) regions of BLG shown in Figure 2c of main text). (b) Lineshape analysis of 2D peak of β (D1), showing characteristic lineshape for AB-BLG.

We have correlated the sSNOM contrasts to the Raman spectroscopic analysis results. Spectra (around G and 2D peaks) of BLG obtained from the b (D1 region) and a (D2 region) in Figure 2c.

The peak intensity ratios of G and 2D peaks of BLG (I_G/I_{2D}), and the lineshapes of 2D-peaks are used to assess the stacking orders in BLG. We estimated the stacking angle and stacking order in BLG from the peak height ratio (I_G / I_{2D}), based on Chen et al's report, in which they correlated the stacking angle and the I_G / I_{2D} . In particular, the AB-BLG has the fixed ratio of $I_G/I_{2D} \approx 1$ ¹⁻³. For AB-BLG, the 2D peaks show characteristic shoulders in 2D peaks, which can be decomposed into four peaks, representing four-step Stokes–Stokes double-resonance Raman (DRR) scattering⁴.

Detailed 2D-lineshapes of AB-BLG show significant differences among reported results^{1, 3, 5, 6} possibly due to the differences in the doping levels of BLG. The most evident feature that distinguishes AB and AA'-BLG is simply the width of 2D peak. For a AA'-BLG with stacking-angle $\theta = 0 \sim 10^\circ$, additional peak at 1625 cm^{-1} (called R'-peak) appears, which provides additional information on stacking angle. For the particular BLG shown in Figure 2 in main text, the I_G / I_{2D} , 2D-peak lineshape, and presence / absence of R'-peak (see Figure S2) indicates the existence of AB-BLG and AA'-BLG with $\theta = 8 \pm 1^\circ$. In the last column of Figure S1, we have provided stacking angles of several other AA'-BLG domains we have examined with sSNOM.

C. Point-dipole modeling for IR s-SNOM

The details of point-dipole sSNOM model can be found in the reports by Aizpurua et al⁷ and Kim et al⁸. Briefly, the tip-end, which is modeled as a nanosphere has a polarizability of:

$$\alpha = 4\pi\alpha^3(\varepsilon_{tip} - \varepsilon_1)/(\varepsilon_{tip} + 2\varepsilon_1), \quad (1)$$

where the ε_{tip} , and ε_1 are dielectric constants of tip-end, and vacuum, respectively. For the calculation of sSNOM amplitude, we evaluate the Fresnel coefficient of graphene / SiO₂ / Si sample:

$$r_p = \frac{Z_1 C - Z_2 S - \sigma_r \pi \alpha C}{Z_1 C + Z_2 S + \sigma_r \pi \alpha C}, \quad (2)$$

where $C = \cos \varphi - i \frac{Z_2}{Z_1} \sin \varphi$, $S = -i \sin \varphi + \frac{Z_2}{Z_1} \cos \varphi$ and $\varphi = k_{2z} d$. The $Z_i = \frac{2\pi}{\lambda} \cdot \frac{\varepsilon_i}{k_{iz}}$ are the

admittance of $i = 1$ (vacuum), 2 (SiO₂), and 3 (Si) media, and the k_{iz} are the out-of-plane wave-

vectors in i 'th media: $k_{iz}(q) = \sqrt{\varepsilon_i(\omega/c)^2 - q^2}$ ($\text{Im}[k_{iz}] > 0$ and $\text{Re}[k_{iz}] > 0$) where q and ω are the in-plane photon momentum vector and angular frequency of light, respectively. The σ_r is the in-plane optical conductivity of graphene, σ , normalized by unit conductivity, $\sigma_0 = c\alpha/4$. The α is the fine-structure constant. Overall far-field scattering amplitude is calculated as:

$$\vec{E}_{scat} \propto \vec{\alpha} \cdot \vec{E}_{inc} (1 - \vec{\alpha} \cdot \vec{G}(\{\sigma, \varepsilon_i\}))^{-1}, \quad (3)$$

where \vec{E}_{inc} is the incident electric field. The \vec{G} is the Green dyadic operator, which is a function of optical conductivities of graphene (σ), and dielectric constants of substrate materials (ε_i). In the s-SNOM measurement, the signal is processed through a lock-in amplifier. The transfer-function between the E_{scat} and the demodulated signal s_n is:

$$s_n = |s_n| e^{i\phi_n} = \frac{1}{2\pi} \int_0^{2\pi} E_{scat,p}(z + \delta z \cos\psi) e^{in\psi} d\psi, \quad (4)$$

where z and δz are average tip-sample distance, and the amplitude of vertical tip-oscillation, respectively.

In the numerical sSNOM modeling, dielectric constant of SiO₂ and Si is obtained by Sellmeier equations.⁹ The tip (PtIr) is made of an alloy of Pt: Ir = 70:30. In the model, the tip is assumed to be a nanosphere with pure Pt with $\varepsilon = -144+75i$ at 0.366 eV and $-1324+916i$ at 0.124 eV^{10,11}. In the model, the tip is assumed to be a nanosphere with an effective radius of a , and this does not necessarily reflect the actual radius of curvature of the tip-end. As such, we treat the radius of curvature (a), average tip-sample distance (z_0), and tip-oscillation amplitude (δz) as fitting parameters. The tip parameters are chosen such that it gives the best match to the

experimental sSNOM intensities of AB-BLG at ω_1 and ω_2 , and the same parameters are used for the calculation of sSNOM intensities of AA-BLG at the two photon energies. For the model calculation shown in main text, we use tip radius as 20 nm, minimum tip-sample distance as 12 nm and tip oscillation amplitude as 35 nm.

D. Intensity and phase contrasts of sSNOM images of BLG

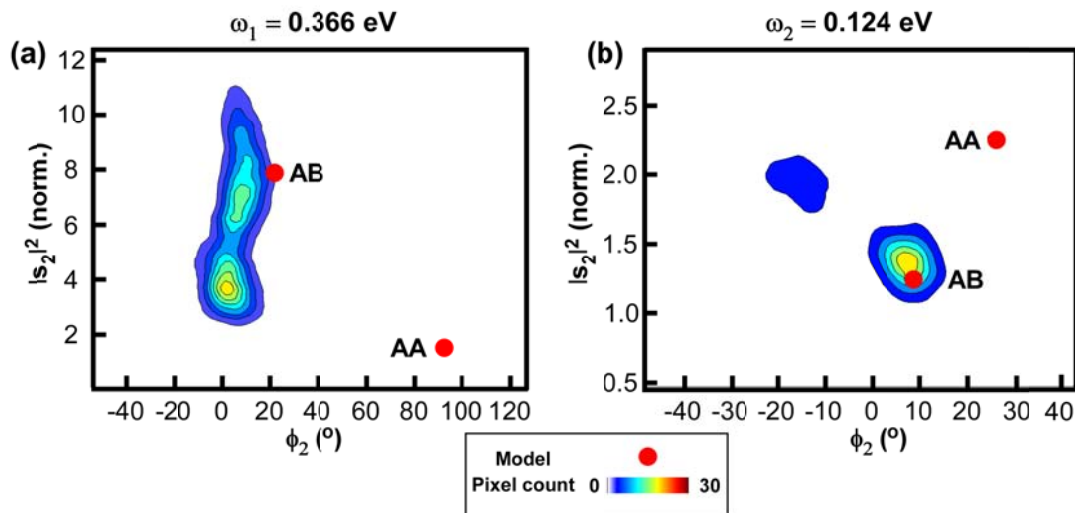


Figure S3. 2-dimensional intensity-phase ($|s_2|^2$ vs ϕ_2) histograms of sSNOM images (Figure S1i~l) at ω_1 and ω_2 frequencies, along with sSNOM model of AB-BLG and AA-BLG (red dots). The intensity and phase contrasts of AB-BLG domain can be satisfactorily reproduced by the model, whereas the phase contrasts of AA'-BLG cannot be reproduced by the model that is based on the optical conductivity of AA-BLG.

Corresponding Author

Zee Hwan Kim, Department of Chemistry, Seoul National University, Seoul, 151-742, Korea

E-mail: zhkim@snu.ac.kr

Author Contributions

‡These authors contributed equally.

Reference

1. C. C. Lu, Y. C. Lin, Z. Liu, C. H. Yeh, K. Suenaga and P. W. Chiu, *ACS Nano*, 2013, **7**, 2587-2594.
2. X. D. Chen, W. Xin, W. S. Jiang, Z. B. Liu, Y. Chen and J. G. Tian, *Adv. Mater.*, 2016, **28**, 2563.
3. S. Sahoo, R. Palai and R. S. Katiyar, *J. Appl. Phys.*, 2011, **110**, 044320.
4. D. H. Yoon, H. R. Moon, Y.-W. Son, G. Samsonidze, B. H. Park, J. B. Kim, Y. P. Lee and H. S. Cheong, *Nano Lett.*, 2008, **8**, 4270–4274.
5. C.-H. Yeh, Y.-C. Lin, P. K. Nayak, C.-C. Lu, Z. Liu, K. Suenaga and P.-W. Chiu, *Journal of Raman Spectroscopy*, 2014, **45**, 912-917.
6. A. C. Ferrari, J. C. Meyer, V. Scardaci, C. Casiraghi, M. Lazzeri, F. Mauri, S. Piscanec, D. Jiang, K. S. Novoselov, S. Roth and A. K. Geim, *Physical Review Letters*, 2006, **97**, 187401.
7. J. Aizpurua, T. Taubner, F. J. de Abajo, M. Brehm and R. Hillenbrand, *Opt. Express*, 2008, **16**, 1529-1545.
8. D.-S. Kim, H. Kwon, A. Y. Nikitin, S. Ahn, L. Martín-Moreno, F. J. García-Vidal, S. Ryu, H. Min and Z. H. Kim, *ACS Nano*, 2015, **9**, 6765-6773.
9. D. C. D. M. Bass, J. Enoch, V. Lakshminarayanan, G. Li, C MacDonal, V Mahajan, E. Van Stryland, *Handbook of Optics*, McGraw-Hill, New York, 2009.
10. E. D. Palik, *Handbook of Optical Constants*, CRC press, 1998.
11. M. J. Weber, *Handbook of Optical Materials*, 2003.